AAPS PharmSciTech, Vol. 11, No. 2, June 2010 (© 2010)
DOI: 10.1208/s12249-010-9422-z

Research Article

Development and *In Vitro* Characterization of Galactosylated Low Molecular Weight Chitosan Nanoparticles Bearing Doxorubicin

Nitin K. Jain[1] and Sanjay K. Jain[1,2]

Received 12 September 2009; accepted 5 April 2010; published online 23 April 2010

Abstract. The aim of the present research was to evaluate the potential of galactosylated low molecular weight chitosan (Gal-LMWC) nanoparticles bearing positively charged anticancer, doxorubicin (DOX) for hepatocyte targeting. The chitosan from crab shell was depolymerized, and the lactobionic acid was coupled with LMWC using carbodiimide chemistry. The depolymerized and galactosylated polymers were characterized. Two types of Gal-LMWC(s) with variable degree of substitution were employed to prepare the nanoparticles using ionotropic gelation with pentasodium tripolyphosphate anions. Factors affecting nanoparticles formation were discussed. The nanoparticles were characterized by transmission electron microscopy and photon correlation spectroscopy and found to be spherical in the size range 106–320 nm. Relatively higher percent DOX entrapment was obtained for Gal-LMWC(s) nanoparticles than for LMWC nanoparticles. A further increase in drug entrapment was found with nanoparticles prepared by Gal-LMWC with higher degree of substitution. A hypothesis which correlates the ionic concentration of DOX in nanoparticles preparation medium and percent DOX entrapment in cationic polymer has been proposed to explain the enhanced DOX entrapment. *In-vitro* drug release study demonstrated an initial burst release followed by a sustained release. The targeting potential of the prepared nanoparticles was assessed by *in vitro* cytotoxicity study using the human hepatocellular carcinoma cell line ($HepG_2$) expressing the ASGP receptors on their surfaces. The enthusiastic results showed the feasibility of Gal-LMWC(s) to entrap the cationic DOX and targeting potential of developed Gal-LMWC(s) nanoparticles to $HepG_2$ cell line.

KEY WORDS: doxorubicin; HCC targeting; low molecular weight chitosan; nanoparticles.

INTRODUCTION

The two commonest malignant primary tumors of the liver are hepatocellular carcinoma (HCC) and cholangiocarcinoma. The former is ten times common than cholangiocarcinoma and is one of the commonest malignant primary neoplasms worldwide. HCC is the fourth commonest neoplasm in the world and the third commonest cause of cancer-related death (1). The HCC puts huge burden on society.

Advances have been made in the management of HCC; the therapies currently available are (a) surgical interventions, including, tumor resection and liver transplantation; (b) percutaneous interventions, including, ethanol injection and radiofrequency thermal ablation, *etc.*; (c) transarterial interventions, including, embolization and chemoembolization; (d) radiation therapy, and (e) systemic therapy including drugs as well as gene and immune therapies. Only surgical resection and liver transplantation are curative therapies during the early stage of disease. They are possible in only 30% of the patients, namely those diagnosed with small tumor burden (2). Except for a few cancer types (e.g., breast cancer) for which hormonal therapy or immunotherapy is used, cytotoxic drugs remain the major form of chemotherapy for cancer. In HCC, chemotherapy can be used as potential neoadjuvant and adjuvant approaches to prevent the spread of cancer cells in patients waiting for liver transplantation and to reduce the chances of recurrence of hepatocellular carcinoma after liver transplantation or successful surgical resection, respectively. Resistance to chemotherapy is a major obstacle in HCC treatment. The mechanisms involved in drug resistance are complex and multifactorial and may be due to inadequate drug exposure or alterations in the cancer cell itself (3). Situation worsens with the poor specificity and high toxicity of chemotherapeutic drugs to the normal cells. Unfortunately, systemic chemotherapy lacks efficacy for HCC, and there is currently no standard treatment for patients with nonresectable HCC (4). Treatment with the drug doxorubicin has provided the best results so far for HCC patients with inoperable tumors. In a meta-analysis, chemoembolization with doxorubicin was shown to improve survival of patients with advanced HCC (5). Unfortunately, fewer than 20% of patients respond to treatment with doxorubicin. This is due to dose-related severe toxicity of doxorubicin (cardiac toxicity, myelosuppression, and dose-limiting toxicity with leucopenia) and the development of multidrug resistance with overexpression of P-gp in tumor cells, which can lead to a marked decrease in drug sensitivity. In fact, the drug doxorubicin is

[1] Pharmaceutics Research Projects Laboratory, Department of Pharmaceutical Sciences, Dr. Hari Singh Gour Vishwavidyalaya, Sagar, Madhya Pradesh 470003, India.
[2] To whom correspondence should be addressed. (e-mail: drskjainin@yahoo.com)

metabolized principally in liver and eliminates primarily via liver and biliary system; still its undesirable access to other organs results in dreaded toxic effects, which ultimately results in discontinuation of therapy.

Targeting of existing chemotherapeutic agents to cancer cells could not only provide specificity but also spare normal cells from the unwanted toxic side effects. Ligand-mediated targeting is one of the most exciting areas in which the site-specific delivery of the drugs can be further improved by entrapping the drug in the ligand-anchored carrier. These ligands include antibodies, glycolipids, glycoproteins, polysaccharides, proteins, and immunoregulatory molecules (6,7). Recent interest has been focused on developing nanoscale delivery vehicles capable of controlling the release of chemotherapeutic agents directly inside cancer cells (8). Various novel and targeted drug delivery systems including nanoparticles and liposomes have been reported to overcome multidrug resistance (MDR) phenomena occurring at both the cellular and the noncellular level, and the results are well documented with anti-tumor drugs such as doxorubicin (9). Nanoparticles loaded with drug demonstrated effective treatment of a number of chemotherapy refractory tumors in animal models (10) and with doxorubicin nanoparticles, encouraging results were obtained at cellular level with reversion of MDR phenomenon (11,12). In liver, various receptors are present on parenchymal and nonparenchymal cells. Parenchymal liver cells, the hepatocytes, are the only cells that possess large numbers of high-affinity cell-surface asialoglycoprotein receptors (ASGPRs) that can bind asialoglycoproteins (ASGP). ASGP possess clustered galactose residues for recognition and binding by ASGP receptors (13).

Cationic natural polymer chitosan was selected for preparation of nanoconstructs. Chitosan is extensively used in drug delivery applications owing to its excellent biocompatibility, biodegradability, low immunogenicity, and biological activities (14). Chitosan is biocompatible with living tissues since it does not cause allergic reactions and rejection. It breaks down slowly to harmless products (amino sugars), which are completely absorbed by the human body (15).

Therefore, it is aimed to develop and characterize nanoparticles of chitosan and its derivatives bearing doxorubicin to evolve an effective means for management of HCC.

MATERIALS AND METHODS

Materials. Chitosan was provided by Central Marine Fisheries Research Institute, Kochi, India. Doxorubicin hydrochloride was generously provided by M/s Khandalwal Labs, Mumbai, India. 1-Ethyl-3-(3-dimethyl-aminopropyl)-carbodiimide (EDC) and N,N,N′,N″-tetramethylethylenediamine (TEMED) buffer solution were purchased from Himedia, India. Lactobionic acid (LA) and pentasodium tripolyphosphate (TPP) were obtained from Sigma, India. All the chemicals were of analytical grade and were used without further purification.

Depolymerization of Chitosan. High molecular weight chitosan (minimum 85% deacetylated) was depolymerized using potassium persulfate (16). Briefly, chitosan (2 g) was taken in 200 ml of 0.5% *v/v* aqueous acetic acid solution, in a three-necked flat bottom flask. The environment inside the flask was purged with nitrogen, and the flask was maintained at 60°C on a magnetic stirrer at 100 rpm speed. Subsequently, potassium persulfate (0.8 mM) was added to the solution, and reaction was allowed to continue for 2 h. Then, alcohol was added to reaction mixture to get the precipitated low molecular weight chitosan (LMWC). Supernatant was discarded, and the precipitate was redissolved in deionized water. The resultant solution was dialyzed using 12-kDa cutoff dialysis membrane overnight. Finally, the dialyzed solution of LMWC was lyophilized to get the LMWC powder.

Characterization of Chitosan and LMWC. The pH-dependent solubility of native chitosan and LMWC was evaluated by turbidity measurement technique (17), where the turbidity of polymer was measured at 600 nm on changing the pH of the solution. Infrared spectra of the native chitosan and LMWC were recorded on a Fourier transform infrared spectrophotometer using the potassium bromide (KBr) disk technique. The ratio of KBr to polymer was 100:1. Degree of deacetylation (DD) of native chitosan and LMWC was calculated by elemental analysis (18). Viscosity average molecular weight (M_v) of the native chitosan and LMWC was determined by viscometry (19). Different concentrations of polymer solution (0.05%, 0.1%, 0.15%, 0.2%, and 0.25% *w/v*) were prepared in 2% *v/v* acetic acid and 0.2 M sodium acetate buffer solution. The relative viscosities were measured with Ostwald viscometer at 30±2°C, and specific viscosities were calculated. The reduced viscosity was calculated for different concentrations of polymer using the specific viscosity data. The intrinsic viscosity was obtained by extrapolating the reduced viscosity on reduced viscosity *vs.* concentration plot to zero concentration as the intrinsic viscosity is defined as:

$$[\eta] = (\eta_{red})c \to 0 \tag{1}$$

The intercept on the abscissa of reduced viscosity *vs.* concentration plot is intrinsic viscosity. The viscosity average molecular weight (M_v) was calculated by using the Mark–Houwink's equation:

$$[\eta] = KM_v^{\alpha} \tag{2}$$

where $[\eta]$ is the intrinsic viscosity of polymer, K and α are constants for given buffer system and polymer. For chitosan, they are influenced by the degree of deacetylation, pH, and ionic strength of the solvent, and their values are $K = 1.64 \times 10^{-30} \times DD$ and $\alpha = -1.02 \times 10^{-2} \times DD$ (20), where DD is degree of deacetylation.

Galactosylation of LMWC. Method reported by Gao et. al. (21)was followed for galactosylation of LMWC. In brief, 0.25 g of polymer was taken in a conical flask and dissolved in 10 ml of 10 mM TEMED buffer solution, and pH was adjusted to 4.7. To this solution, 0.450 g of EDC was added, and the resultant solution was kept on magnetic stirrer at 25°C for 24 h. Different quantities of LA [0.179 g (0.5 mmol) and 0.268 g (0.75 mmol)] were added to this solution. Both solutions were stirred for another 72 h at 25°C on magnetic stirrers. After 72 h of stirring, resulting Gal-LMWC(s) were dialyzed (12-kDa cutoff dialysis membrane) for 4 days against Milli-Q water, and finally, the purified Gal-LMWC(s) were lyophilized.

Characterization of Gal-LMWC(s). The Gal-LMWC(s) were characterized using infrared spectroscopy, and the degree of substitution was determined by elemental analysis data.

Preparation and Optimization of Doxorubicin-Loaded Gal-LMWC(s) and LMWC Nanoparticles

Nanoparticles of Gal-LMWC(s) and LMWC were prepared using the ionotropic gelation technique (22). In brief, the Gal-LMWC(s) were first dissolved in aqueous acetic acid solution at various concentrations (0.05%, 0.1%, 0.2%, and 0.3% *w/v*). The concentration of acetic acid in aqueous was, in all cases, 1.5 times higher than that of Gal-LMWC(s). Then, the TPP was dissolved in purified water at various concentrations (0.2, 0.4, 0.6, 0.8, and 1.0 mg/ml). The solution of Gal-LMWC(s) (10 ml) was kept on mechanical stirrer (100 rpm) under continuous stirring at room temperature and the TPP solution (4 ml) was added into Gal-LMWC(s) solutions to obtain the nanoparticles of Gal_1-LMWC and Gal_2-LMWC, respectively.

For the incorporation of doxorubicin HCl into the nanoparticles, the aqueous solution of drug was added in Gal-LMWC(s) solution, and the solution was kept under occasional magnetic stirring for 30 min at room temperature and then TPP solution was added dropwise under mechanical stirring. The physical changes occurring in the solution was observed and the solution turned into opalescence suspension was considered as the colloidal dispersion containing nanoparticles. The nanoparticle suspension was subjected to ultracentrifugation at 20,000 rpm at 10°C for 30 min and supernatant was discarded and pellet containing nanoparticles was resuspended in saline phosphate buffer (pH 7.4) before being subjected to further analysis and applications. Similarly, the nanoparticles of LMWC were prepared.

Process and formulation variables viz. polymer/TPP concentration, drug concentration, and stirring speed were identified and optimized. Finally, the nanoparticles were prepared using the optimized parameters and characterized.

Particle Shape, Size, and Zeta Potential. The shape and surface morphology of nanoparticles were investigated using transmission electron microscopy (Philips CM-10). The particle size, polydispersity index, and zeta potential of prepared formulations were determined using photon correlation spectroscopy (Zetasizer Nano ZS) after dispersing the nanoparticles in PBS (pH 7.4).

Percent Drug Entrapment and Loading Capacity. Percent drug entrapment and loading capacity were determined after separation of nanoparticles from the medium containing non-entrapped drug by ultracentrifugation at 20,000 rpm at 10°C for 30 min. The amount of free drug was determined by UV-visible spectroscopy at 481 nm. The supernatant of unloaded nanoparticles was used as basic correction. The percent encapsulation efficiency (EE) was calculated as follows

$$\mathrm{EE} = (A - B)/A \times 100 \quad (3)$$

A: total amount of doxorubicin hydrochloride added, *B*: free amount of doxorubicin hydrochloride in supernatant.

The LC was calculated from the equation

$$\%\ \mathrm{LC} = (A - B)/C \times 100 \quad (4)$$

A: total amount of doxorubicin hydrochloride added, *B*: free amount of doxorubicin hydrochloride in supernatant, *C*: nanoparticles weight.

In Vitro Drug Release Study. The lyophilized nanoparticles (10 mg) were dispersed in 10 ml of PBS (pH 7.4), and the particulate suspension was then placed in a dialysis membrane bag with a molecular cutoff 5 kDa. The bag was tied and submerged in 150 ml of PBS solution. The whole system was maintained at 37±1°C under continuous magnetic stirring (75 rpm) and was protected from light. At appropriate time interval, 2 ml of the diffusion medium was removed and replaced immediately with 2 ml of fresh PBS (pH 7.4). The amount of doxorubicin released in the withdrawn medium was quantified by UV spectrophotometer at 481 nm.

Cytotoxicity assay. The cytotoxicity of doxorubicin-loaded nanoparticles was determined against HepG2 cells. Free drug, drug-loaded Gal-LMWC(s), and LMWC nanoparticles were studied to assess their cell growth inhibition potential employing a tetrazolium dye (MTT) assay (23). $HepG_2$ cells were cultured in 75 ml tissue culture flask in 10 ml of Dulbecco's Modified Eagle's Medium (DMEM) with 10% fetal bovine serum, 100 IU/ml penicillin, and 100 µg/ml streptomycin at 37°C in humidified atmosphere of 5% CO_2 and maintained in a log-phase growth at about $3–6\times10^5$ cells/ml. After 7 days of cell culture, the cells were harvested with 0.05% trypsin. Cells were collected and the cell number counted using hemocytometer, then diluted into cell suspension at a density of 1×10^5 cells/ml by further addition of DMEM medium, and seeded into 96-well plate at 100 µl/well. After being cultured for 24 h in carbon dioxide incubator, the cells were immediately treated with increasing doses of selected formulations containing DOX and increasing concentration of DOX solution in PBS (pH 7.4) and incubated for another 48 h. DOX-loaded formulations were also added with excess amount of galactose. Control cells were also cultured at the same time. MTT assay was performed, and percentage cell viability was determined by measuring the absorbance at 540 nm using ELISA plate reader (24). The cell viability was calculated as the percentage of MTT absorbance as follows:

$$\%\text{Cell Viability} = \text{Mean experimental absorbance}/\text{Mean control absorbance} \times 100 \quad (5)$$

RESULTS

Preparation and Characterization of LMWC. At low concentration (0.1% and 0.2% *w/v*), the LMWC is soluble over a wide pH range whereas the solubility of native chitosan was high at acidic pH but abruptly deceased at pH, a little over neutrality (data not shown). On contrary to native chitosan, which is practically insoluble in pH range 6–8, the LMWC was found fairly soluble in the solutions of pH 6–8. The experimental DD value of native chitosan and LMWC was obtained 87% and 85%, respectively. The intrinsic viscosities were found to be 126.66 and 22.35 ml/g for chitosan and LMWC, respectively. The viscosity average molecular weight of native chitosan was found to be ≈120 kDa and for LMWC, it was ≈21 kDa.

Preparation and Characterization of Galactosylated LMWC. The LMWC (Mv≈21 kDa) was coupled with LA containing a galactose residue via an active ester intermediate using EDC. Fifty to sixty percent yield of Gal-LMWC(s) was obtained. The IR spectrum of lactobionic acid exhibited a broad absorption occurring in the region 3,400–2,400 cm^{-1} showing the presence of –OH group and a distinctive band at 1,740 cm^{-1} shows the carbonyl stretching (C=O) of carboxylic groups. In the IR spectra of Gal-LMWC(s), the disappearance of the carbonyl stretching of lactobionic acid is observed, which could be due to the amide bond formation between carboxylic groups of lactobionic acid and the amine group of LMWC (Fig. 1). In elemental analysis, the C/N weight percent was found 6.334 and 6.665 for Gal_1-LMWC and Gal_2-LMWC, respectively. Degree of substitution was calculated as 10.6% and 14.1% for Gal_1-LMWC and Gal_2-LMWC, respectively.

Preparation and Characterization of Nanoparticles. Various concentrations of Polymer [Gal-LMWC(s) and LMWC] and TPP were employed to observe the ratios of polymer to TPP, which form the nanoparticles. Three phenomena, viz. solution, opalescent suspension, and aggregate formation, occurred. Further, to ensure the formation of nanoparticles, the opalescent suspensions were observed under transmission electron microscope to differentiate the nanoparticles from aggregates.

Higher concentration of LMWC in comparison to TPP resulted in no change in LMWC solution as occurred with formulations LCN_1, LCN_6, LCN_7, LCN_{11}, LCN_{12}, LCN_{16}, LCN_{17}, and LCN_{18}. Similar concentration of Gal-LMWC(s) to TPP resulted in no change in Gal-LMWC(s) solution as occurred with formulations G_1CN_6, G_1CN_{11}, G_1CN_{12}, G_1CN_{16}, G_1CN_{17}, G_2CN_6, G_2CN_{11}, G_2CN_{12}, G_2CN_{16}, and G_2CN_{17}.

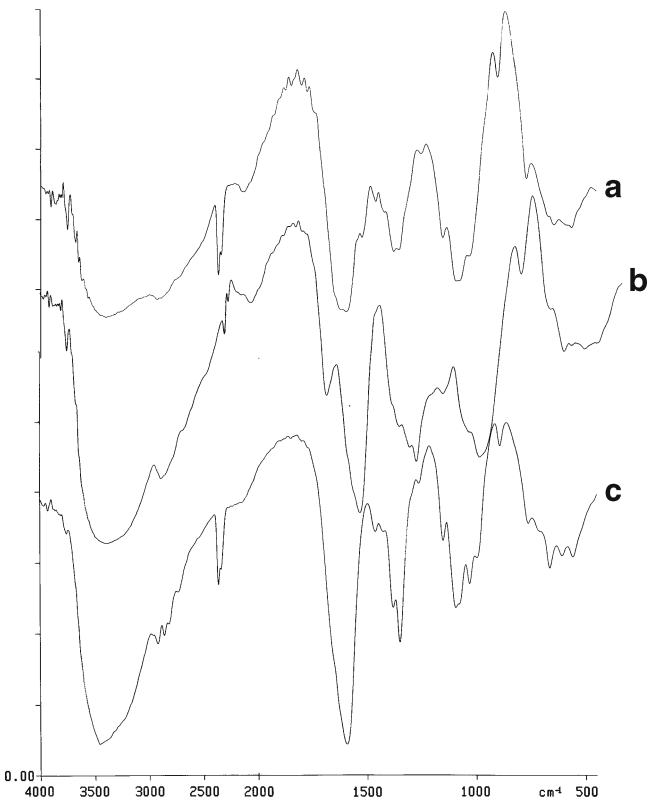

Fig. 1. IR spectrum of **a** low molecular weight chitosan, **b** lactobionic acid, and **c** Gal_2-LMWC

The formation of aggregates was observed after microscopic analysis of a few formulations. The particle size range for nanoparticles was found to be 91.24±3.47 to 331.92±14.87 nm for LMWC, 92.48±2.15 to 338.75±11.84 nm for Gal_1-LMWC, and 94.16±3.27 to 340.84±10.15 nm for Gal_2-LMWC. The effect of polymer concentration on drug entrapment efficiency was studied (Table I). Low drug entrapment (2.12±3.29–5.24± 0.32%) was observed with 0.05% of polymer. Effect of TPP concentration on drug entrapment was found to be minimal.

The effect of drug concentration on the percent drug entrapment efficiency in LMWC and Gal-LMWC(s) nanoparticles was studied. Higher drug encapsulation efficiency was achieved with 1.5 mg/ml drug concentration in case of Gal-LMWC(s) nanoparticles prepared by 0.1% *w/v* concentration of polymer (Table II). The further increase in drug concentration to 2.0 mg/ml resulted in no remarkable change in drug encapsulation efficiency. The relatively higher percent drug entrapment was obtained for Gal-LMWC(s) nanoparticles than for LMWC nanoparticles prepared on similar formulation and process parameters.

In optimization of stirring speed, it was observed that for 0.1% and 0.2% *w/v* concentrations of polymer the nanoparticles obtained at 200 rpm were having highest drug entrapment efficiency whereas for the polymer concentration of 0.3% *w/v* 300 rpm stirring speed produced optimized formulation. At higher speed (300 rpm), no effect was observed on percent drug entrapment efficiency, but reduction in particle size was seen for 0.3% *w/v* polymer concentration. Nanoparticle formulations exhibiting highest percent drug entrapment for a particular concentration of polymer were selected as optimized formulation.

The formulations were prepared from LMWC, Gal_1-LMWC, and Gal_2-LMWC using the optimized parameters (Table III). All optimized nanoparticulate formulations bearing drug were characterized for shape and surface morphology, particle size, polydispersity index, zeta potential, percent drug entrapment efficiency, drug loading capacity, *in vitro* drug release study in PBS (pH 7.4), and *in vitro* cytotoxicity study on $HepG_2$ cell line.

Compared with Gal-LMWC(s) nanoparticles, LMWC nanoparticles exhibited relatively smoother surface (Figs. 5, 6 and 7). No conglomeration was seen in photomicrograph, showing that nanoparticles had a very distinct boundary.

In all cases, the particle size of LMWC nanoparticles was lower than the particle size of Gal-LMWC(s) nanoparticles. The particle size of formulations $LCNP_1$–$LCNP_3$ ranged from 98.04±2.47 to 294.32±7.84 nm, for formulations GC_1NP_1–GC_1NP_3, this range was 104.64±4.26 to 319.57±10.23 nm. The formulations GC_2NP_1–GC_2NP_3 exhibited particle size range from 106.16±5.86 to 303.61±12.67 nm. The polydispersity index (PI) was determined for all the formulations, and it was found that the formulations had narrow size distribution with polydispersity index <0.33.

The average zeta potential for LMWC nanoparticles ranged from 34.1 to 55.4 mV. For Gal_1-LMWC and Gal_2-LMWC nanoparticles, it was found to be 21.3 to 39.5 mV and 19.7 to 39.4 mV, respectively.

Gal-LMWC(s) nanoparticles are exhibiting higher drug entrapment than the LMWC nanoparticles. Maximum drug entrapment was obtained for formulations GC_1NP_2 and

Table I. Optimization of Polymer *vs*. TPP Concentration

Polymer Conc. (% *w/v*)	TPP Conc. (mg/ml)	Formulation Code	Visual Analysis	Microscopic Analysis	Drug Entrapment (%)	Particle Size (nm)	Formulation Code	Visual Analysis	Microscopic Analysis	Drug Entrapment (%)	Particle Size (nm)	Formulation Code	Visual Analysis	Microscopic Analysis	Drug Entrapment (%)	Particle Size (nm)
0.05	0.2	LCN_1	S	–	–	–	G_1CN_1	OS	– (NP)	4.22±0.13	93.64±2.15	G_2CN_1	OS	– (NP)	5.13±0.21	96.26±3.49
	0.4	LCN_2	OS	– (NP)	2.04±0.18	91.24±3.47	G_1CN_2	OS	– (NP)	4.42±0.26	92.48±2.15	G_2CN_2	OS	– (NP)	5.24±0.32	94.16±3.27
	0.6	LCN_3	OS	– (NP)	2.12±3.29	91.63±3.29	G_1CN_3	OS	AG	–	–	G_2CN_3	OS	AG	–	–
	0.8	LCN_4	OS	AG	–	–	G_1CN_4	OS	AG	–	–	G_2CN_4	OS	AG	–	–
	1.0	LCN_5	AG (PPT)	–	–	–	G_1CN_5	AG (PPT)	–	–	–	G_2CN_5	AG (PPT)	-	–	–
0.1	0.2	LCN_6	S	–	–	–	G_1CN_6	S	–	–	–	G_2CN_6	S		–	–
	0.4	LCN_7	S	–	–	–	G_1CN_7	OS	– (NP)	14.34±0.12	108.45±2.13	G_2CN_7	OS	– (NP)	15.87±0.54	109.14±3.14
	0.6	LCN_8	OS	– (NP)	5.24±0.13	99.23±2.61	G_1CN_8	OS	– (NP)	14.82±0.41	107.95±3.12	G_2CN_8	OS	– (NP)	16.04±0.62	109.06±4.32
	0.8	LCN_9	OS	– (NP)	5.26±0.11	98.67±3.42	G_1CN_9	OS	– (NP)	14.69±0.67	106.43±2.89	G_2CN_9	OS	– (NP)	16.12±0.85	107.86±2.94
	1.0	LCN_{10}	OS	– (NP)	5.26±0.15	98.12±2.76	G_1CN_{10}	OS	– (NP)	14.86±0.64	105.65±2.36	G_2CN_{10}	OS	– (NP)	16.11±0.21	106.80±3.18
0.2	0.2	LCN_{11}	S	–	–	–	G_1CN_{11}	S	–	–	–	G_2CN_{11}	S	–	–	–
	0.4	LCN_{12}	S	–	–	–	G_1CN_{12}	S	–	–	–	G_2CN_{12}	S	–	–	–
	0.6	LCN_{13}	OS	– (NP)	7.82±0.32	120.79±5.29	G_1CN_{13}	OS	– (NP)	25.12±0.62	127.26±6.18	G_2CN_{13}	OS	– (NP)	27.25±0.43	128.65±4.18
	0.8	LCN_{14}	OS	– (NP)	8.07±0.29	119.24±2.61	G_1CN_{14}	OS	– (NP)	25.32±0.27	125.23±3.25	G_2CN_{14}	OS	– (NP)	27.27±0.52	126.24±3.27
	1.0	LCN_{15}	OS	– (NP)	8.05±0.37	118.42±5.17	G_1CN_{15}	OS	– (NP)	25.32±0.38	122.42±5.86	G_2CN_{15}	OS	– (NP)	27.31±0.37	123.16±4.15
0.3	0.2	LCN_{16}	S	–	–	–	G_1CN_{16}	S	–	–	–	G_2CN_{16}	S	–	–	–
	0.4	LCN_{17}	S	–	–	–	G_1CN_{17}	S	–	–	–	G_2CN_{17}	S	–	–	–
	0.6	LCN_{18}	S	–	–	–	G_1CN_{18}	AG (PPT)	–	–	–	G_2CN_{18}	AG (PPT)	–	–	–
	0.8	LCN_{19}	AG (PPT)	–	–	–	G_1CN_{19}	OS	AG	–	–	G_2CN_{19}	OS	AG	–	–
	1.0	LCN_{20}	OS	– (NP)	7.69±0.33	331.92±14.87	G_1CN_{20}	OS	– (NP)	19.57±0.43	338.75±11.84	G_2CN_{20}	OS	– (NP)	20.84±0.35	340.84±10.15

Values are expressed as mean±SD, n=3. Polymer: 10 ml, TPP: 4 ml, stirring speed: 100 rpm and stirring time: 15 min, drug concentration: 1.0 mg/ml (2 ml)
OS opalescent suspension, *AG* aggregates, *S* solution, *PPT* precipitate, *NP* nanoparticles

Table II. Optimization of Drug Concentration

Polymer Conc. (% *w/v*)	Drug Conc. (mg/ml)	Formulation Code	Drug Entrapment (%)	Particle Size (nm)	Formulation Code	Drug Entrapment (%)	Particle Size (nm)	Formulation Code	Drug Entrapment (%)	Particle Size (nm)
0.1	1.0	LCD_1	5.26±0.15	98.12±2.76	G_1CD_1	14.86±0.64	105.65±2.36	G_2CD_1	16.11±0.21	106.80±3.18
0.2		LCD_2	8.05±0.37	118.42±5.17	G_1CD_2	25.32±0.38	122.42±5.86	G_2CD_2	27.31±0.37	123.16±4.15
0.3		LCD_3	7.69±0.33	331.92±14.87	G_1CD_3	19.57±0.43	338.75±11.84	G_2CD_3	20.84±0.35	340.84±10.15
0.1	1.5[a]	LCD_4	5.24±0.26	98.72±4.18	G_1CD_4	15.63±0.28	106.32±3.74	G_2CD_4	18.95±0.41	107.35±5.17
0.2		LCD_5	8.09±0.38	118.63±4.27	G_1CD_5	27.29±0.58	126.57±5.54	G_2CD_5	32.31±1.12	132.14±8.49
0.3		LCD_6	7.72±0.35	332.95±9.62	G_1CD_6	20.82±0.66	340.96±17.91	G_2CD_6	21.36±0.57	343.45±13.14
0.1	2.0	LCD_7	5.41±0.37	99.13±2.64	G_1CD_7	15.65±0.45	106.48±3.78	G_2CD_7	18.94±0.21	107.39±4.45
0.2		LCD_8	7.86±0.31	119.13±5.27	G_1CD_8	27.25±0.62	127.06±6.12	G_2CD_8	32.22±0.43	132.21±6.18
0.3		LCD_9	7.63±0.27	331.74±5.82	G_1CD_9	20.58±0.72	341.13±15.41	G_2CD_9	21.37±0.15	343.56±14.17

Values are expressed as mean ± SD, $n=3$. TPP: 1 mg/ml, stirring speed: 100 rpm and stirring time: 15 min, [a] Shows the optimized parameter

GC_2NP_2, as 27.72±1.02% and 32.42±0.82%, respectively. While with same process and formulation parameters the $LCNP_2$ formulation show 8.27±0.27% drug entrapment. The drug loading capacity (LC) of formulations $LCNP_1$, $LCNP_2$, and $LCNP_3$ was found to be 3.98%, 3.46%, and 3.02%, respectively. For formulations GC_1NP_1, GC_1NP_2, GC_1NP_3, GC_2NP_1, GC_2NP_2, and GC_2NP_3, the LC was found to be 9.68%, 10.72%, 4.54%, 10.09%, 11.12%, and 4.27%, respectively. *In vitro* drug release profile of prepared formulations was determined in PBS, pH 7.4 (Fig. 2).

The formulations $LCNP_2$, GC_1NP_2, GC_2NP_2, and GC_2NP_3 were selected to assess the *in vitro* cytotoxicity on $HepG_2$ cell line. The results of the cytotoxicity study were presented in the form of percent viable cells remain after treatment with the formulations containing drug, doxorubicin hydrochloride. The results revealed that the formulations GC_1NP_2 and GC_2NP_2 exhibited remarkable cytotoxicity activity on the $HepG_2$ cell line. The percent viability of $HepG_2$ cells after treatment with above said formulations was found to be 14.12±0.97% and 11.23±0.78%, respectively, after incubating the cell with formulations containing 10 μg/ml concentration of doxorubicin hydrochloride, whereas the percent viability for same concentration of drug solution was found to be 28.72±0.54%. Formulation GC_2NP_3 also exhibited higher cell viability and was appeared less effective than the plain drug solution with 42.72±2.14% cell viability. The cell viability for the formulation GC_2NP_2 after 24 h of incubation was 10.25±0.56, while in the presence of galactose, the cell viability was found to be 42.38±4.95% for same formulation (Fig. 3). The reduction in the IC_{50} value for $HepG_2$ cells was observed for doxorubicin-loaded nanoparticles in comparison to doxorubicin solution. The IC_{50} values for formulations GC_1NP_2 and GC_2NP_2 were found to be 3.97 and 3.86 μg/ml, which are significantly less than the IC_{50} for the drug solution (5.98 μg/ml).

DISCUSSION

Attempts have been made to deliver the drug specifically to liver cells for efficient and effective treatment of liver diseases by applying nanoparticulate and vesicular formulations (25). However, none of them is liver-specific or cell type-specific since the majority of carriers administered intravenously are endocytosed by the reticuloendothelial system, the carriers are often found to be highly concentrated in Kupffer cells. Now, it is well established that the Kupffer cell count in HCC decreased as HCC becomes less differentiated (3). Another cellular target for achieving the hepatic targeting of anticancer could be hepatic endothelial cells, but these cells could be the suitable candidate for targeting the antiangiogenic drugs not for cytotoxic drugs, and also, the sinusoidal endothelial cell dysfunction is regarded as the initial event of liver injury (26). As HCC is cancer of liver parenchymal cells, hence the delivery of most widely used anticancer drug, doxorubicin hydrochloride into liver parenchymal cells is important to achieve maximum therapeutic index of drug. The ASGPRs that are present only on sinusoidal surface of hepatocytes offer one of most promising receptor site since they exhibit high affinity and a rapid

Table III. Optimized Formulations

Formulation Code	Polymer Conc. (%w/v)	Stirring Speed	Drug Entrapment (%)[a]	Particle Size (nm)[a]	LC[b]	PI[b]	Zeta Potential[b]
$LCNP_1$	0.1	200	5.83±0.27	98.04±2.47	3.98	0.23	34.1
$LCNP_2$	0.2	200	8.27±0.27	116.38±5.41	3.46	0.29	45.1
$LCNP_3$	0.3	300	8.78±0.39	294.32±7.84	3.02	0.11	55.4
G_1CNP_1	0.1	200	15.92±0.51	104.64±4.26	9.68	0.27	21.3
G_1CNP_2	0.2	200	27.72±1.02	121.73±5.78	10.72	0.21	27.8
G_1CNP_3	0.3	300	21.36±0.82	319.57±10.23	4.54	0.14	39.5
G_2CNP_1	0.1	200	19.42±0.56	106.16±4.82	10.09	0.25	19.7
G_2CNP_2	0.2	200	32.42±0.82	128.08±5.16	11.12	0.20	23.1
G_2CNP_3	0.3	300	21.86±0.47	303.61±12.67	4.27	0.09	39.4

TPP: 1 mg/ml
[a] Values are expressed as mean ± SD, $n=3$
[b] Average value of three observations

internalization (27). Efficient *in vivo* targeting to ASGPRs of hepatocytes has been described using asialoglycoprotein, asialo-oromucoid, mannose, fucose, or galactose conjugates (28). Nanoparticulate formulations appended with galactose moiety could exploit the increased expression of ASGPRs in HCC *in vivo*.

Chitosan is a polysaccharide containing four elements in its formula, its cationicity, and the consequent capacity to form polyelectrolyte complexes and nitrogen derivatives, according to the chemistry of the primary amino groups make it suitable to couple with appropriate ligand thereby achieving the intracellular drug delivery by the developed formulation (29). LMWC is fairly soluble in neutral aqueous media and its advantage is ease of modification, useful as gene or peptide drug carriers and drug carriers, and the particles with smaller diameter can be obtained with LMWC (21). In present study, chitosan was depolymerized using potassium persulfate (KPS), which produced the LMWC in short time with homogenous product (16). A free radical degradation mechanism of chitosan with KPS was explained (30).

The higher solubility of LMWC at low concentration (0.1–0.2% *w/v*) over a wide range of pH is attributed to decreased intermolecular interaction, such as van der Waals forces and the lower molecular weight. On contrary to native chitosan, which is practically insoluble in pH range 6–8, the LMWC was found fairly soluble in the solutions of pH 6–8. The solubility of LMWC in aqueous pH 7 could be attributed to its low molecular weight, which lowers the intermolecular attraction forces between the LMWC molecules (17).

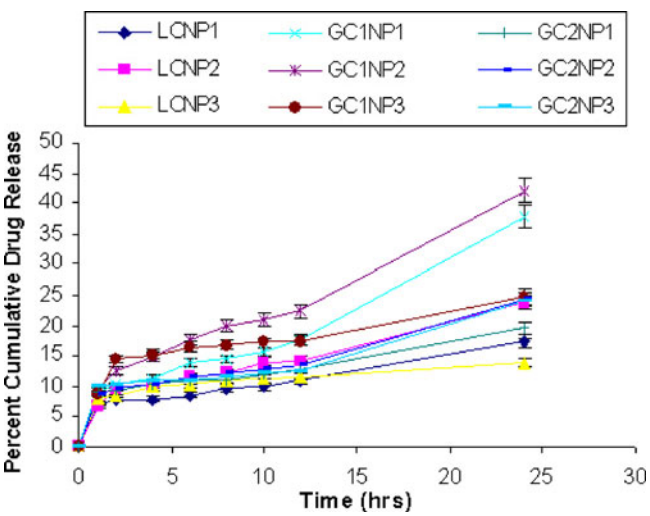

Fig. 2. *In vitro* release profile of LMWC and Gal-LMWC(s) nanoparticles

The infrared spectroscopy analysis of LMWC clearly shows that the process has no remarkable influence on the structure. DD of chitosan can affect the zeta potential and uptake capacity of the nanoparticles (31). No change in DD is observed after depolymerization of chitosan. It is reported that, if there are great changes in the DD, there will be remarkable changes in the absorption bands 3,253 and 3,143 cm^{-1} (32), but in our case, no such changes were observed in IR spectra. The viscosity average molecular weight for chitosan and LMWC was determined by viscometry method (19). It was found that the molecular weight of native chitosan reduced approximately one sixth after persulfate depolymerization.

The LA, bearing a galactosyl group, is usually used as a recognition moiety for the hepatocyte-targeting carrier (33). LA was coupled with LMWC using carbodiimide chemistry. Carbodiimides are used to mediate the formation of amide linkages between a carboxylate and an amine or phosphoramidate linkage between a phosphate and an amine (34). The synthesis of Gal-LMWC(s) was confirmed by infrared spectroscopy. In the IR spectra of Gal-LMWC(s), the disappearance of the carbonyl stretching of lactobionic acid is observed, which could be due to the amide bond formation between carboxylic groups of lactobionic acid and the amine group of LMWC. A slight shift of all peaks of amide I and amide II of Gal-LMWC(s) is an indication of the conformational change of LMWC after reaction with lactobionic acid. The –OH stretching of Gal-LMWC(s), which appeared at around 3,400 cm^{-1} in LMWC shifted to higher wave number, which indicates that the intermolecular hydrogen bonding between Gal-LMWC(s) chains increased due to introduction of lactobionic acid into the chitosan. Compared with IR spectrum of LMWC (Fig. 1), Gal-LMWC showed a new signal at 1,667 cm^{-1}, which is assigned to acylamino group, and the strong peak around 1,150 cm^{-1} in Gal-LMWC(s) is suggesting the successful introduction of galactosyl unit to LMWC. The DS was calculated using percent C/N ratio found in elemental analysis. With the increase in the amount of molar ratio of LA to glucosamine unit, percent C/N in Gal-LMWC(s) increased which shows that there is increment in DS.

Chitosan nanoparticles/microspheres may be prepared by the chemical cross-linking agent, glutaraldehyde combined

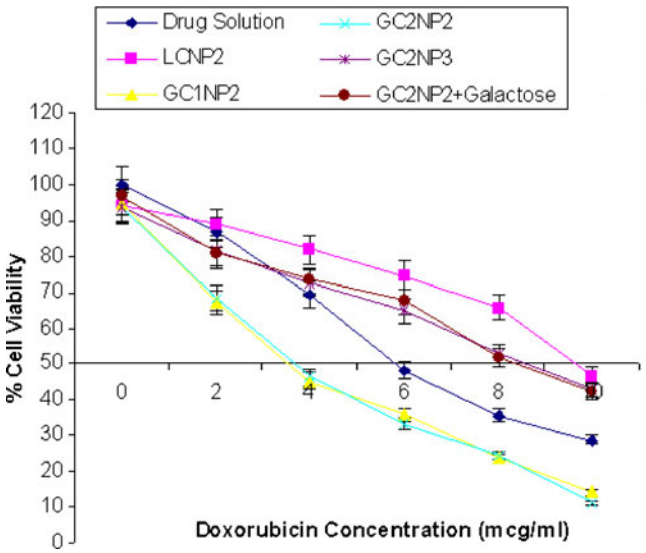

Fig. 3. Percent cell viability *vs.* doxorubicin concentration

with emulsion technique (35), coacervation/precipitation technique (36), spray-drying technique (37), reverse micellar technique (38), and emulsion droplet coalescence technique (39). A physical method, ionotropic gelation, was followed because of its simplicity and the use of mild conditions for preparation of nanoparticles. This technique offers reversible physical cross linking by electrostatic interaction, thereby avoiding the possible toxicity of reagent and other undesirable effects (29). Various anions, sulfate, citrate, and TPP, may be used for cross-linking process, but because of more charge numbers and higher charge density (40), TPP gives more spherical shape to the bed; therefore, TPP was used. In a study, chitosan nanoparticles produced by the ionic gelation of chitosan and TPP were studied with their diameter ranging between 20 and 200 nm (41).

Various concentrations of polymer [Gal-LMWC(s) or LMWC] and TPP were used to observe the ratios of polymer to TPP, which form the nanoparticles. It was observed that when various concentration of TPP is added to polymer solution in aqueous acetic acid, three phenomena, viz. solution, opalescent suspension, and aggregate formation, occurred. The zone of opalescent suspension should correspond to a suspension of very small particles because of Tyndall effect. To ensure the formation of nanoparticles, the opalescent suspensions were observed under transmission electron microscope to differentiate the nanoparticles from aggregates. All opalescent suspensions were not found as nanoparticles. It shows that the formation of nanoparticles is affected by polymer and TPP concentration. Very higher concentration of polymer resulted in no change in polymer solution. This could be due to insufficient availability of polyanion to crosslink with the excess protonated amino group present with polymer.

Increasing the concentrations of polymers from 0.05% to 0.3% resulted in increase in drug entrapment efficiency up to 0.2% *w/v* concentration and then decreased drug entrapment efficiency was obtained for 0.3% *w/v* concentration of polymer. The low entrapment efficiency obtained with 0.05% of polymers could be due to complete protonation of amino group of polymers at acidic pH, thereby the polymer chain tends to occupy maximum space in solution due to repulsion of intra- and intermolecular amino groups. Thus, polymer chains attain maximum stretching and linearity at this low concentration. Further, the weakly basic drug, doxorubicin hydrochloride (p*K*a=8.22) is ionized in aqueous acidic solution, which creates repulsion between the drug and polymer and the drug molecule could find ample space to stabilize itself far apart. Therefore, 0.05% *w/v* concentration of polymers was not taken in to consideration in further studies.

Low drug entrapment was obtained for all concentrations of LMWC, which could be due to cationic nature of polymer and drug. During the incorporation of doxorubicin hydrochloride in polymeric nanoparticles, the repulsion between the drug and cationic polymer was anticipated; therefore, the aqueous acetic solutions of polymer was kept with drug for 30 min to effect the diffusion of positively charged drug in to the cationic strings of LMWC and Gal-LMWC(s). These strings were interpreted as worm-like single chains of chitosan (42). The slight increase in drug entrapment on increasing the LMWC concentration from 0.1% to 0.2% *w/v* could be due to availability of relatively more LMWC chains, which could hold relatively more drugs within polymeric network. Further, increase in LMWC concentration did not increase in doxorubicin entrapment. The higher concentration of LMWC (0.3% *w/v*) provides highly viscous solution, which could decrease encapsulation of doxorubicin and gelation between LMWC and TPP. The sharp increase in drug entrapment efficiency for Gal-LMWC(s) concentration 0.2% could be due to availability of lactobionic acid substituted polymer chain in extended polymeric network. The low drug entrapment efficiency for Gal-LMWC(s) concentration 0.3% (*w/v*) suggested that the drug could not be distributed in viscous solution effectively.

Effect of TPP concentration on the encapsulation efficiency was found to be negligible. It was experienced that increase of TPP concentration was of benefit to keep the spherical shape of nanoparticles rather than affecting the drug entrapment process.

The increase in polymer concentration led to increase in particle size of nanoparticles. The effect was found much pronounced with 0.3% *w/v* polymers that could be due to increased adhesivity of the polymer at this concentration. The particle size for Gal-LMWC(s) nanoparticles was found to be relatively higher than the particle size of LMWC nanoparticles which could be due to substitution of some amino group of LMWC by bulky lactobionate moiety and higher drug entrapment.

The effect of drug concentration on the percent drug entrapment efficiency was studied. The change in drug concentration did not increase the percent drug entrapment of LMWC nanoparticles. On contrary, marginal increase in drug encapsulation efficiency was found (from 25.32±0.38% to 27.29±0.58%) on increasing the drug concentration from 1.0 to 1.5 mg/ml in case of Gal_1-LMWC nanoparticles. The further increase in drug concentration to 2.0 mg/ml resulted in no change in drug encapsulation efficiency.

Very low percent drug entrapment in LMWC nanoparticles was obtained, which could be due to repulsion between drug and LMWC strings. It is, therefore, assumed that the LMWC nanoparticles did allow only small quantity of drug to be retained within the particle, likely by physical

entrapment, which could be effected by polymer concentration, not by drug concentration. In a similar study, the quite low drug entrapment (9.1%) was obtained for chitosan nanoparticles (24).

The relatively higher percent drug entrapment was obtained for Gal-LMWC(s) nanoparticles which was still higher for Gal_2-LMWC nanoparticles. The findings could be explained after reviewing the structure of chitosan in aqueous acidic solution. It has been shown that the structures of chitosan in solution consisted of a number of roughly spherical agglomerates intercalated with very thin straightened fibers. These chains can be considered as block-type copolymers, composed of blocks of almost 100% acetylated polysaccharide intercalated with blocks of highly deacetylated chain (43). The deacetylated chains are fully stretched by the electrostatic repulsion among the $–NH_3^+$ groups and the acetylated blocks are micelle-like agglomerates because of the hydrophobic forces. The micelle size of 17.96 nm with chain length of 209.5 nm was observed in TEM photomicrograph of uranyl stained chitosan (44). On the basis of these findings, it is hypothesized that the acetylated unit of polymers [LMWC and Gal-LMWC(s)] could be present as micelles in aqueous solutions of polymers and deacetylated unit makes the intercalated chain. In Gal-LMWC(s), some of the $–NH_3^+$ ($–NH_2$) groups of LMWC have been substituted by lactobionate moiety. Hence, the Gal-LMWC(s) posses positively charged amino group along with nearly neutral/negatively charged lactobionate moiety in the form of strings or chain and N-acetyl-β-D-glucosamine unit could be present as micelle-like agglomerates intercalated by stretched chain. The higher percent drug entrapment in Gal-LMWC(s) nanoparticles could be due to the entry of positively charged drug into N-acetyl-β-D-glucosamine micelle via lactobionate unit, where the ionic drug could experience minimum repulsion. The movement of drug toward these micelles could stabilize the positively charged drug in cationic polymer solution. Moreover, the still higher percent drug entrapment was obtained with Gal_2-LMWC polymer, which could be due to the higher degree of substitution of $–NH_2$ by lactobionate moiety, which could provide more pathways for the movement of drug into N-acetyl-β-D-glucosamine micelle.

The low drug entrapment for 1.0 mg/ml concentration of drug could be due to lesser movement of drug into micelles due to rather weaker ionic repulsion between drug and polymer and drug and drug (Fig. 4, Scheme I). It is expected that at 1.5 mg/ml drug concentration the ionic repulsion is more and the more drug move toward micelles to gain stability, which resulted in maximum drug entrapment. On further increasing the drug concentration to 2.0 mg/ml did not increase percent drug entrapment which could be due to the limited capacity of the micelles to withhold the positively charged drug, and there could also be possibility of repulsion between drug entering into the micelle and drug that had already entered in the micelle or the establishment of an ionic equilibrium between the drug ions present in micelle and drug ions present in aqueous solution (Fig. 4, Schemes II and III). It is proposed that modulating the DD and DS of LMWC can further increase the entrapment efficiency of positively charged drug in Gal_1-LMWC and Gal_2-LMWC.

The formulations were prepared using the optimized parameters (Table III) and characterized for various parameters. Compared with Gal-LMWC(s) nanoparticles, LMWC nanoparticles exhibited relatively smoother surface. This could be due to the presence of bulky lactobionate moiety on the surface of nanoparticles prepared by Gal-LMWC(s). No conglomeration was seen in photomicrograph, showing that nanoparticles had a very distinct boundary (Figs. 5, 6, 7).

The order of particle size for nanoparticulate formulations of three polymers was found as Gal_2-LMWC nanoparticles >Gal_1-LMWC nanoparticles >LMWC nanoparticles at 0.1% and 0.2% *w/v* concentrations of polymers. This could be due to the similar order of entrapment efficiency of the formulations. The other reason for the increment of particle size might be the substitution of amino group of LMWC by bulky LA. It was found that the formulations had narrow size distribution with polydispersity index <0.33. The small PI value indicated a homogenous dispersion of all nanoparticulate formulations. All prepared formulations exhibited positive zeta potential, which explained the cationic nature of the LMWC and synthesized Gal-LMWC(s). The positive zeta potential of chitosan nanoparticles was reported in several studies (45,46). In all cases, the zeta potential of LMWC nanoparticles was found to be higher than the Gal-LMWC(s)

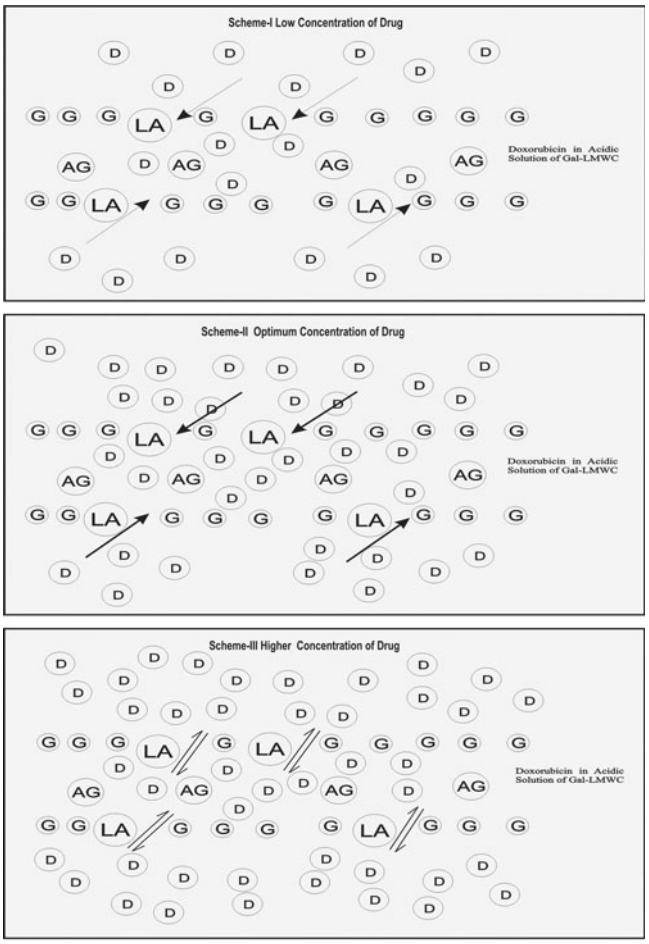

Fig. 4. Schematic representation of hypothesized mechanism of doxorubicin entrapment in cationic polymer (Gal-LMWC). Top: Scheme-I; Middle: Scheme-II; Bottom: Scheme-III

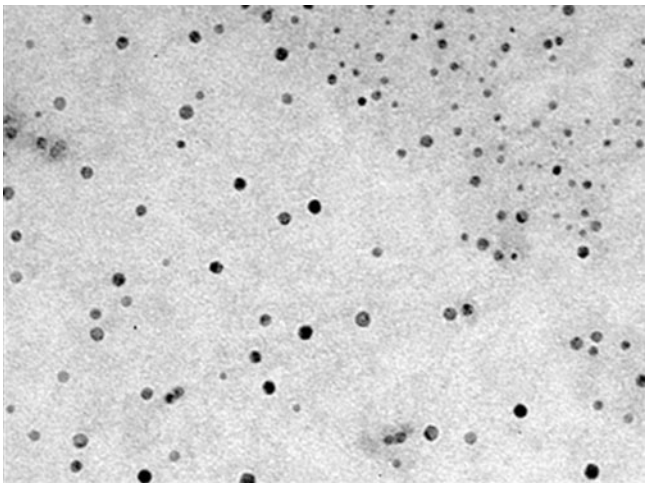

Fig. 5. TEM of blank LMWC nanoparticles

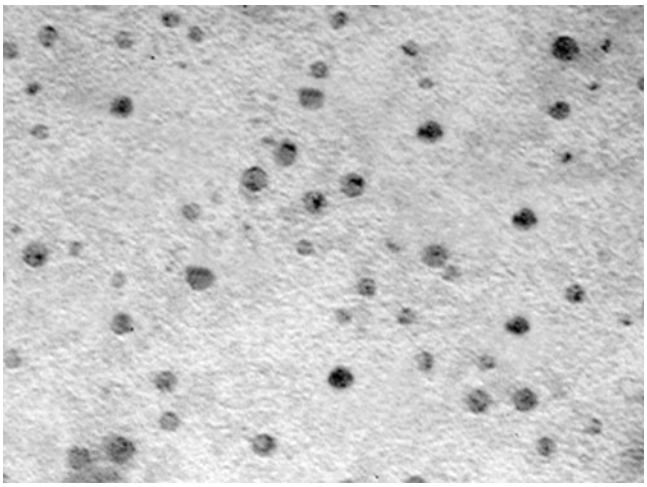

Fig. 7. TEM of drug-loaded Gal_1-LMWC nanoparticles

nanoparticles for a definite concentration of polymer and TPP, which could be due to presence of more numbers of positively charged amino groups on nanoparticles surface.

The percent doxorubicin hydrochloride entrapment efficiency in nanoparticles prepared with 0.1% and 0.2% concentration of Gal-LMWC(s) was found to be fairly good. The LC of the nanoparticles was found to be affected by the polymer concentration. Low LC was found for formulations GC_1NP_3 and GC_2NP_3 which could be due to low percent drug entrapment efficiency of formulations and higher particle size of nanoparticles. On increasing the concentration of LMWC, the LC was decreased, while for Gal-LMWC(s), the LC was found to be marginally increased, which could be due to increased drug entrapment.

In vitro drug release profiles of doxorubicin-loaded LMWC and Gal-LMWC(s) nanoparticles showed the initial phase of release, which is attributed to the drug located/adsorbed at the cross-linked surface of the nanoparticles. The release rate data showed that relatively higher amount of drug is adsorbed on surface of Gal-LMWC(s) nanoparticles as the percent release rate after 1 h is higher. This could be due to adsorption of doxorubicin on cross-linked nanoparticulate surface, porous nature of polymers, and substitution of positively charged amino groups by LA. After initial release of 6–10% of drug, which could be the surface-associated drug, the remaining unreleased doxorubicin was assumed to be well entrapped within the polymeric nanoparticles. Relatively slow release was observed in subsequent time (Fig. 2), which was quite distinct from the profiles obtained from chitosan nanoparticles encapsulating insulin, where 100% release was observed within 15 min (47). This could be due to concealment of drug in micelles present in Gal-LMWC(s) nanoparticles. The cumulative percent drug release is very less for LMWC nanoparticles, and it is expected that degradation of LMWC would be required for accomplishing the release process. To confirm this hypothesis, enzymatic digestion of nanoparticles is required but the process could degrade doxorubicin as well, hence it was not performed. A study showed that the drug release from microspheres involves two different mechanisms, i e., drug molecules diffusion and polymer matrix degradation (48). Since the size of doxorubicin molecule is much smaller than that of nanoparticles, doxorubicin hydrochloride molecules diffuse easily through the surface or the pore of nanoparticles. Higher cumulative release rate was obtained with some Gal-LMWC(s) formulations prepared by low concentration of TPP, which could be due to low cross linking of Gal-LMWC(s) nanoparticles.

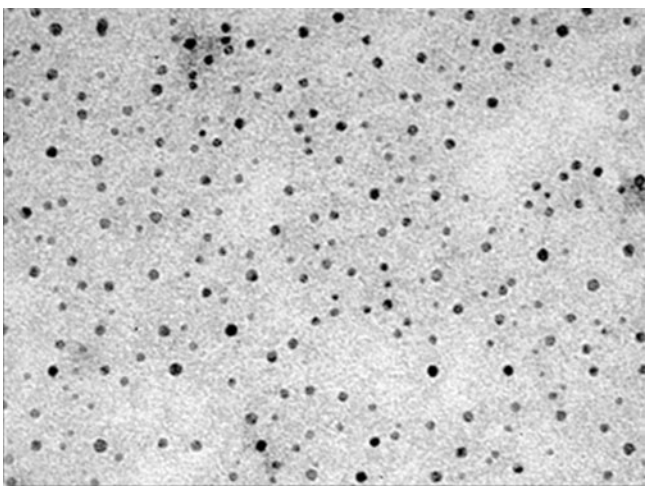

Fig. 6. TEM of blank Gal_1-LMWC nanoparticles

The cytotoxicity potential of the selected formulations was studied using MTT assay (49). The ability of cells to reduce MTT provides an indication of mitochondrial integrity and activity, which in turn, may be interpreted as a measure of viability and/or cell number (32). The formulations $LCNP_2$, GC_1NP_2, GC_2NP_2, and GC_2NP_3 were selected to assess the *in vitro* cytotoxicity on $HepG_2$ cell line. $HepG_2$ cell line is human hepatocellular carcinoma cell line expressing the ASGP receptors on their surfaces. The results of the cytotoxicity study were presented in the form of percent viable cells remains after treatment with blank formulations and the formulations containing drug. The higher percent viability of $HepG_2$ cells was observed with formulation $LCNP_3$ which could be due to the sustained release of drug from the formulation. Similarly formulation GC_2NP_3 also exhibited higher cell viability and was appeared less effective than the plain drug solution with 42.72±2.14% cell viability. The

reasons could be larger size of particles (373.58±12.18 nm), which is not suitable for the occurrence of cell death via RME and more sustained release of drug from the nanoparticles. Given the limited *in vitro* drug release exhibited by the formulations GC_1NP_2 and GC_2NP_2, it is hypothesized that the cytotoxic action exhibited by these liganded carriers could be due to endocytosis, rather than the release of free drug in the cell culture medium. Further, to examine whether for Gal-LMWC(s) nanoparticles are taken up by the asialoglycoprotein receptors, the competitive inhibition experiments were performed. The cell viability of $HepG_2$ cells was found to be markedly increased for formulations GC_2NP_2 when it was incubated with an excess of galactose, suggesting both formulations are effectively taken up by asialoglycoprotein receptors in $HepG_2$ cells. A significant reduction in the IC_{50} value for $HepG_2$ cells was observed for doxorubicin-loaded nanoparticles in comparison to doxorubicin solution. Our study suggests that the positively charged doxorubicin could be well entrapped in Gal-LMWC(s) nanoparticles and the developed formulation could selectively deliver the doxorubicin to hepatic parenchymal cells.

ACKNOWLEDGMENT

Authors are thankful to Central Drug Research Institute, Lucknow, India and Jawaharlal Nehru Cancer Hospital, Bhopal, India for providing necessary facility to carry out this research work.

REFERENCES

1. Ann P. Looking at liver cancer. Nursing. 2006;36:52–5.
2. Bruix J, Sherman M, Llovet JM, Beaugrand M, Lencioni R, Burroughs AK *et al.* Clinical management of hepatocellular carcinoma. Conclusions of the Barcelona-2000 EASL conference. European Association for the Study of the Liver. J Hepatol. 2001;35:421–30.
3. Liu J, Williams RO. Long-term stability of heat-humidity cured cellulose acetate phthalate coated beads. Eur J Pharm Biopharm. 2002;53:167–73.
4. Llovet JM, Bruix J. Systematic review of randomized trials for unresectable hepatocellular carcinoma: chemoembolization improves survival. Hepatology. 2003;37:429–42.
5. Baird RD, Kaye SB. Drug resistance reversal—are we getting closer? Eur J Cancer. 2003;39:2450–61.
6. Molema G, Meijer DKF. Targeting of drugs to various blood cell types using (neo-) glycoproteins, antibodies and other protein carriers. Adv Drug Deliv Rev. 1994;14:25–50.
7. Meijer DKF, Jansen RW, Molema G. Drug targeting systems for antiviral agents: options and limitations. Antivir Res. 1992;18: 215–58.
8. Gu FX, Karnik R, Wang AZ, Alexis F, Levy-Nissenbaum E, Hong S *et al.* Targeted nanoparticles for cancer therapy. Nanotoday. 2007;2:14–21.
9. Muggia FM, Hainsworth JD, Jeffers S. Phase II study of liposomal doxorubicin in refractory ovarian cancer: antitumor activity and toxicity modification by liposomal encapsulation. J Clin Oncol. 1997;15:987–93.
10. Cuvier C, Roblot-Treupel L, Millot JM, Lizard G, Chevillard S, Manfait M *et al.* Doxorubicin-loaded nanospheres bypass tumor cell multidrug resistance. Biochem Pharmacol. 1992;44:509–17.
11. De Colin VAC, Dubernet C, Nemati F, Soma E, Appel M, Ferte J *et al.* Reversion of multidrug resistance with polyalkylcyanoacrylate nanoparticles: towards a mechanism of action. Br J Cancer. 1997;76:198–205.
12. Bennis S, Chapey C, Robert J, Couvreur P. Enhanced cytotoxicity of doxorubicin encapsulated in polyisohexylcyanoacrylate nanospheres against multidrug-resistant tumour cells in culture. Eur J Cancer. 1994;30:89–93.
13. Ashwell G, Morell AG. The role of surface carbohydrates in the hepatic recognition and transport of circulating glycoproteins. Adv Enzymol Relat Areas Mol Biol. 1974;41:99–128.
14. Sarasam AR, Krishnaswamy RK, Madihally SV. Blending chitosan with polycaprolactone: effects on physicochemical and antibacterial properties. Biomacromolecules. 2006;7:1131–8.
15. Nicol S. Life after death for empty shells. New Sci. 1991; 129:46–8.
16. Tharanathan RN, Prashanth KVS 2001. Indian patent, 433/DEL/01.
17. Kubota N, Tatsumoto N, Sano T, Toya K. Simple preparation of half N-acetylated chitosan highly soluble in water and aqueous organic solvents. Carbohydr Res. 2000;324:268–74.
18. Xu J, McCarthy SP, Fross RA, Kaplan DL. Chitosan film acylation and effects on biodegradability. Macromolecules. 1996;29:3436–40.
19. Pantaleone D, Yalpani M, Scollar M. Preparation of methyl 2, 3-di-O-mesyl-4, 6-thioanhydro-alpha-D-galactopyranoside and methyl 2-O-mesyl-4, 6-thioanhydro-alpha-D-gulopyranoside. Carbohydr Res. 1992;237:325–32.
20. Wang W, Bo S, Li S, Qin W. Determination of the Mark–Houwink equation for chitosans with different degrees of deacetylation. Int J Biol Macromol. 1991;13:281–5.
21. Gao S, Chen J, Xu X, Zhi D, Yang Y, Hua Z *et al.* Galactosylated low molecular weight chitosan as DNA carrier for hepatocyte-targeting. Int J Pharm. 2003;255:57–68.
22. Vila A, Sanchez A, Janes K, Behrens I, Kissel T, Vila JL *et al.* Low molecular weight chitosan nanoparticles as new carriers for nasal vaccine delivery in mice. Eur J Pharm Biopharm. 2004;57:123–31.
23. Truter EJ, Santos AS, Els WJ. Assessment of the antitumour activity of targeted immunospecific albumin microspheres loaded with cisplatin and 5-fluorouracil: toxicity against a rodent ovarian carcinoma *in vitro*. Cell Biol Int. 2001;25:51–9.
24. Janes KA, Fresneau MP, Marazuela A, Fabra A, Alonso MJ. Chitosan nanoparticles as delivery systems for doxorubicin. J Control Release. 2001;73:255–67.
25. Yoshida M, Yamamoto N, Uehara T, Terao R, Nitta T, Harada N *et al.* Kupffer cell targeting by intraportal injection of the HVJ cationic liposome. Eur Surg Res. 2002;34:251–9.
26. Braet F, Wisse E. Structural and functional aspects of liver sinusoidal endothelial cell fenestrae: a review. Comp Hepatol. 2002;1:1–17.
27. Kim TH, Jiang HL, Nah JW, Cho MH, Akaike T, Cho CS. Receptor-mediated gene delivery using chemically modified chitosan. Biomed Mater. 2007;2:S95–100.
28. Kwoh DY, Coffin CC, Lollo CP, Jovenal J, Banaszczyk MG, Mullen P, *et al.* (1999) Stabilization of poly-L-lysine/DNA polyplexes for *in vivo* gene delivery to the liver. Biochim Biophys Acta: Gene Structure and Expression 1444:171–190.
29. Agnihotri SA, Mallikarjuna NN, Aminabhavi TM. Recent advances on chitosan-based micro- and nanoparticles in drug delivery. J Control Release. 2004;100:5–28.
30. Hsu SC, Don TM, Chiua WY. Free radical degradation of chitosan with potassium persulfate. Polym Degrad Stab. 2002; 75:73–83.
31. Huang M, Khor E, Lim L. Uptake and cytotoxicity of chitosan molecules and nanoparticles: effects of molecular weight and degree of deacetylation. Pharm Res. 2004;21:344–53.
32. Mao S, Shuai X, Unger F. The depolymerization of chitosan: effects on physicochemical and biological properties. Int J Pharm. 2004;281:45–54.
33. Park IK, Kim TH, Park YH, Shin BA, Choi ES, Chowdhury EH *et al.* Galactosylated chitosan-graft-poly(ethylene glycol) as hepatocyte-targeting DNA carrier. J Control Release. 2001;76:349–62.
34. Ghosh SS, Kao PM, McCue AW, Chappelle HL. Use of maleimide-thiol coupling chemistry for efficient synthesis of digonucleotide-enzyme conjugate hybridisation probes. Bioconjug Chem. 1990;1:71–6.
35. Kumbar SG, Kulkarni AR, Aminabhavi TM. Crosslinked chitosan microspheres for encapsulation of diclofenac sodium: effect of crosslinking agent. J Microencapsulation. 2002;19:173–80.

36. Mao HQ, Roy K, Troung-Le VL, Janes KA, Lim KY, Wang Y *et al*. Chitosan-DNA nanoparticles as gene carriers: synthesis, characterization and transfection efficiency. J Control Release. 2001;70:399–421.
37. He P, Davis SS, Illum L. Chitosan microspheres prepared by spray drying. Int J Pharm. 1999;187:53–65.
38. Mitra S, Gaur U, Ghosh PC, Maitra AN. Tumour targeted delivery of encapsulated dextran–doxorubicin conjugate using chitosan nanoparticles as carrier. J Control Release. 2001;74:317–23.
39. Tokumitsu H, Ichikawa H, Fukumori Y. Chitosan-gadopentetic acid complex nanoparticles for gadolinium neutron-capture therapy of cancer: preparation by novel emulsion-droplet coalescence technique and characterization. Pharm Res. 1999;16:1830–5.
40. Shu XZ, Zhu KJ. Controlled drug release properties of ionically cross-linked chitosan beads: the influence of anion structure. Int J Pharm. 2002;233:217–25.
41. Xu Y, Du Y. Effect of molecular structure of chitosan on protein delivery properties of chitosan nanoparticles. Int J Pharm. 2003;250:215–26.
42. Berth G, Dautzenberg H, Peter MG. Physico-chemical characterization of chitosans varying in degree of acetylation. Carbohydr Polym. 1998;36:205–16.
43. Aiba SI. Studies on chitosan: 3. Evidence for the presence of random and block copolymer structures in partially N-acetylated chitosans. Int J Bio Macromol. 1991;13:40–4.
44. Pedroni VI, Schulz PC, Gashaider ME, Andreucetti N. Chitosan structure in aqueous solution. Colloid Polym Sci. 2003;282:100–2.
45. Gan Q, Wang T, Cochrane C, McCarron P. Modulation of surface charge, particle size and morphological properties of chitosan-TPP nanoparticles intended for gene delivery. Colloids Surf B Biointerfaces. 2005;44:65–73.
46. Qi LF, Xu ZR, Li Y, Jiang X, Han XY. *In vitro* effects of chitosan nanoparticles on proliferation of human gastric carcinoma cell line MGC803 cells. World J Gastroenterol. 2005;11:5136–41.
47. Fernandez-Urrusuno R, Calvo P, Remunan-Lopez C, Vila JL, Alonso MJ. Enhancement of nasal absorption of insulin using chitosan nanoparticles. Pharm Res. 1999;16:1576–81.
48. Zhou SB, Deng XM, Li XH. Investigation on a novel core-coated microspheres protein delivery system. J Control Release. 2001;75:27–36.
49. Mosmann T. Rapid colorimetric assay for cellular growth and survival: application to proliferation and cytotoxicity assays. J Immunol Methods. 1983;65:55–63.